applied sciences

MDPI

Article

Laccase Immobilization on Poly(*p*-Phenylenediamine)/Fe_3O_4 Nanocomposite for Reactive Blue 19 Dye Removal

Youxun Liu, Mingyang Yan, Yuanyuan Geng and Juan Huang *

School of Basic Medical Sciences, Xinxiang Medical University, Jinsui Avenue 601, Xinxiang 453003, China; liuyouxun@126.com (Y.L.); mingyangyan@126.com (M.Y.); 18790550067@139.com (Y.G.)
* Correspondence: huangjuan@xxmu.edu.cn; Tel.: +86-37-3383-1739

Academic Editor: Raed Abu-Reziq
Received: 5 July 2016; Accepted: 15 August 2016; Published: 17 August 2016

Abstract: Magnetic poly(*p*-phenylenediamine) (P*p*PD) nanocomposite was synthesized via mixing *p*-phenylenediamine solution and Fe_3O_4 nanoparticles and used as a carrier for immobilized enzymes. Successful synthesis of P*p*PD/Fe_3O_4 nanofiber was confirmed by transmission electron microscopy and Fourier transform infrared spectroscopy. Laccase (Lac) was immobilized on the surface of P*p*PD/Fe_3O_4 nanofiber through covalent bonding for reactive blue 19 dye removal. The immobilized Lac-nanofiber conjugates could be recovered from the reaction solution using a magnet. The optimum reaction pH and temperature for the immobilized Lac were 3.5 and 65 °C, respectively. The storage, operational stability, and thermal stability of the immobilized Lac were higher than those of its free counterpart. The dye removal efficiency of immobilized Lac was about 80% in the first 1 h of incubation, while that of free Lac was about 20%. It was found that the unique electronic properties of P*p*PD might underlie the high dye removal efficiency of immobilized Lac. Over a period of repeated operation, the dye removal efficiency was above 90% during the first two cycles and remained at about 43% after eight cycles. Immobilized Lac on P*p*PD/Fe_3O_4 nanofiber showed high stability, easy recovery, reuse capabilities, and a high removal efficiency for reactive blue 19 dye; therefore, it provides an optional tool for dye removal from wastewater.

Keywords: laccase; poly(*p*-phenylenediamine); reactive blue 19; magnetic nanoparticles; removal; dye; wastewater treatment

1. Introduction

Laccase (*p*-diphenol: dioxygen oxidoreductase, EC 1.10.3.2) belongs to the family of copper-containing oxidases, which catalyze the 1-electron oxidation of a wide range of inorganic and organic substances, coupled with a 4-electron reduction of oxygen to water [1–4]. This enzyme is among the most studied redoxases and has been used successfully as a commercial industrial catalyst. Laccase (Lac) has shown many applications in biomedical, biotechnological, and environmental areas such as organic synthesis, wine cork making, teeth whitening, immunoassay analyte labeling, biofuel cells, and biosensors [4–6]. Moreover, Lac can also play a major role in bioremediation processes such as dye removal from wastewater [7,8].

As is widely known, the difficulty of recovering free enzymes from solution and the poor stability of many free enzymes, including Lac, have hindered their development for use in large-scale applications [9]. Accordingly, immobilized enzymes have greater prospects for development since they have higher storage, thermal, and operational stabilities than their free counterparts. Among the carrier materials commonly used for immobilizing enzymes, nanomaterials have attracted great attention due to their large surface area to volume ratio and high porosity, which are highly efficient for enzyme attachment [10,11]. More importantly, the development of various nanostructure carriers for enzyme immobilization facilitates a broader range of applications and an increased efficiency

of immobilized enzymes [12–14]. Furthermore, for some redoxases that require an electron shuttle for their catalytic reaction, their activity can be enhanced when these enzymes are immobilized on electron-conducting carriers. It has been demonstrated that carbon nanotubes are an ideal carrier for redoxase immobilization, since they possess superb electrical conductivity and can effectively enhance direct electron transfer between electrodes and proteins [15,16]. In addition, magnetic polymer-based nanocomposites for enzyme immobilization have also attracted extensive attention since they have shown great potential for applications in enzyme recovery and recycling [10].

Since Lac is a redoxase, it has been speculated that its activity may be enhanced through an electron-transfer pathway between the carrier and the enzyme when it is immobilized on nanostructured materials with good conductivity. Polyaniline and poly(*p*-phenylenediamine) (P*p*PD) nanofibers have a large surface area and a high density of nanopores onto which enzymes can be efficiently absorbed. These nanofibers are also capable of conducting electricity as polymer nanowires. Therefore, they are considered to be excellent candidate materials for enzyme immobilization, especially for redoxases. The use of magnetic and electron-conducting P*p*PD nanofibers as supports for Lac immobilization has the following obvious advantages: (1) the high specific surface area and functional N–H groups of P*p*PD nanofiber are suitable for the efficient binding of Lac; (2) magnetic nanocomposites provide a method for easily separating immobilized enzymes from solutions following treatment, thereby lowering operation costs; (3) conductive P*p*PD nanofibers can provide efficient channels for electron transportation between enzymes and their substrates, which could improve the catalytic activity of Lac.

A wide variety of dyes have been extensively used in many industries such as the pulp, leather, cosmetics, food, paper, and textile industries [17]. Synthetic dyes have harmful effects on the environment owing to their toxicity to microbes, hydrophytes, and animals. Thus, environmental protection acts have been enacted in most countries, which demand that textile waste must be treated before being released into natural water bodies [18]. It has now been proven that Lac can oxidize many synthetic dyes with high efficiency [19,20]. It has been reported that the magnetic P*p*PD nanofiber had been used as a nano-adsorbent for removal of $Cr_2O_7^{2-}$ ions or a photocatalyst for degradation of acid dyes [21,22]. However, to the best of our knowledge, there have not been any reports concerned with the immobilization of Lac on magnetic P*p*PD nanofiber for the removal of dye. In addition, reactive blue 19 (RB19) (Figure 1), which is a typical anthraquinone dye, has been widely used in the textile industry and is a representative of an important class of toxic and recalcitrant organopollutants. Therefore, RB19 was selected as a model recalcitrant compound for removal from solution by enzymatic treatment in this study.

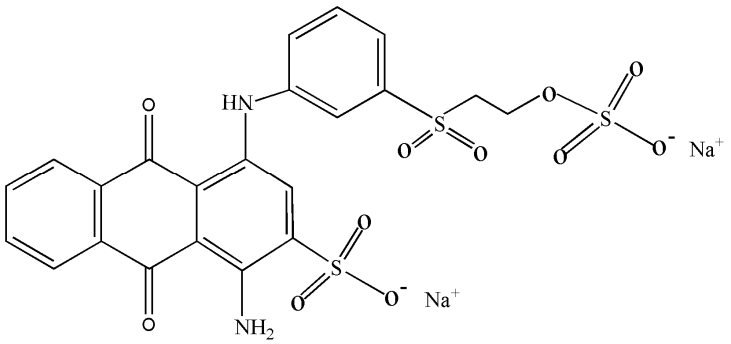

Figure 1. Molecular structure of reactive blue 19.

In this work, we fabricated a magnetically separable P*p*PD/Fe_3O_4 nanocomposite for Lac immobilization to increase enzyme loading, improve enzyme recovery and recycling, and create a surface microenvironment that permits electrical conductivity. The effects of pH and temperature

on Lac activity and stability were studied. The reuse capabilities of Lac and its removal efficiency for RB19 were also determined.

2. Materials and Methods

2.1. Reagents and Materials

p-Phenylenediamine, ferric chloride ($FeCl_3 \cdot 6H_2O$), ferrous chloride ($FeCl_2 \cdot 4H_2O$), ammonium persulfate, reactive blue 19 (RB19), and 2,2′-azinobis-(3-ethylbenzthiazoline-6-sulphonate) (ABTS) were purchased from Sigma-Aldrich (St. Louis, MO, USA). Lac (enzyme activity $\geq$0.6 U/mg) was purchased from Sunson Industry Group (Beijing, China). All chemicals were used as received without further purification. Deionized water was used throughout the whole experiment.

2.2. Synthesis of Magnetic Nanoparticles

Fe_3O_4 nanoparticles were synthesized according to the method described by Cao et al. [23]. Briefly, 1.988 g of $FeCl_2 \cdot 4H_2O$ and 5.46 g of $FeCl_3 \cdot 6H_2O$ in 60 mL deionized water were mixed at room temperature. The mixture was stirred vigorously at 80 °C for 25 min. After that, NH_4OH (20 mL) was quickly added into the mixture until the pH reached 10.0. After 30 min vigorous stirring, the black precipitate was separated by magnetic decantation. The samples were then washed several times with deionized water until a pH value of 7.0 was obtained. The resulting Fe_3O_4 nanoparticles were dried at 60 °C under vacuum for 8 h.

2.3. Synthesis of PpPD/Fe_3O_4 Nanocomposite

In light of the process described by Zhang et al. [24], the nanocomposite of P*p*PD with Fe_3O_4 was prepared by in situ doping polymerization in the presence of H_3PO_4 as a dopant. The overall synthetic pathway for nanocomposite (P*p*PD/Fe_3O_4) is shown in Scheme 1. The synthesis procedure was as follows: 0.3 mL of P*p*PD monomer and 0.05 g of Fe_3O_4 nanoparticles were mixed with H_3PO_4 (1.5 mL) and dissolved in 20 mL of deionized water under supersonic stirring for 10 min at 15 °C. Then, an aqueous solution of ammonium persulfate (0.6 g in 6 mL deionized water) was added to the above solution. The mixture was incubated at room temperature overnight. The formed precipitate was separated by magnetic decantation and then washed with deionized water several times and methanol three times. Finally, the obtained dark precipitate was dried under vacuum at 50 °C for 24 h.

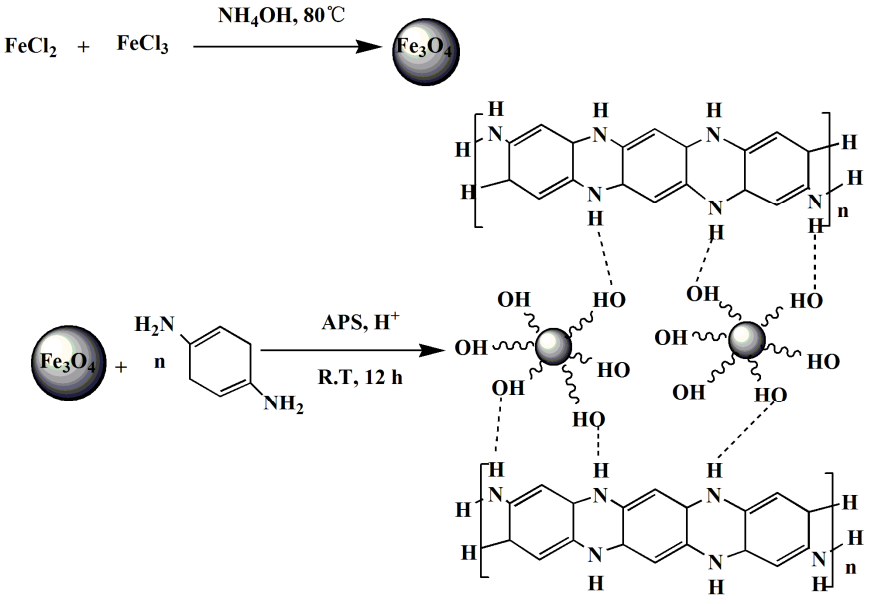

Scheme 1. The synthetic pathway of poly(*p*-phenylenediamine) (P*p*PD)/Fe_3O_4 nanocomposite.

2.4. Immobilization of Lac on PpPD/Fe_3O_4 Nanocomposite

Lac was covalently immobilized onto the P*p*PD/Fe_3O_4 nanocomposite using the glutaraldehyde activation procedure. In this procedure, 50 mg of P*p*PD/Fe_3O_4 nanocomposite was thoroughly washed with phosphate-buffered saline (PBS, 50 mM, pH 7.0). The pretreated carrier was submerged into a glutaraldehyde solution (7%, *v*/*v*), and then vigorously shaken for 4 h. After this, the activated carrier was washed four times with phosphate buffer, and then mixed with a Lac solution (2 mg/mL in PBS, pH 7.0). Enzyme immobilization was conducted at room temperature for 2 h. The resultant Lac-immobilized P*p*PD/Fe_3O_4 nanocomposite was washed with PBS until no Lac activity was detected in the decanted wash solutions.

2.5. Measurement Activity of Free and Immobilized Lac

Assays of free and immobilized Lac activities were conducted spectrophotometrically using ABTS as a substrate [23]. The reaction was initiated by adding 0.1 mL of the Lac solution into 2.7 mL of sodium acetate buffer solution (50 mM, pH 4.0) and 0.2 mL of ABTS (4 mmol/L), and then the mixtures are incubated at 25 °C for 3 min. The increase in absorbance of the solution was recorded at the wavelength of 420 nm. For the measurement activity of immobilized Lac, it was immediately separated from the reaction solution using a magnet after the mixtures were incubated at 25 °C for 3 min. The increase in absorbance of the supernatant was recorded at the wavelength of 420 nm. One unit of enzyme activity is defined as the amount of enzyme required to oxidize 1 μmol of ABTS per min.

2.6. Evaluation of the Effects of pH and Temperature on Lac Activity and Stability

The effects of reaction temperature and substrate pH were investigated by measuring the activities of free and immobilized Lac at a range of temperatures and pH. The stabilities of the immobilized and free Lac were determined as follows. The storage stabilities of the free and immobilized Lac were tested after storage at 4 °C. For the assessment of their thermal stability, free and immobilized preparations of Lac were stored in PBS at 50 °C. The preparations of Lac were withdrawn at the same timed intervals during incubation, and the residual activity of each preparation was measured. For the assessment of its operational stability, the activity of immobilized Lac was measured as follows. After each reaction run, the immobilized Lac was taken out and washed with PBS to remove any residual substrate on the P*p*PD/Fe_3O_4 nanocomposite. The immobilized Lac was then added to a fresh reaction solution and its activity was detected under optimal conditions.

2.7. Electrochemical Analysis

Before modification, a Pt electrode was polished mechanically with 0.03 μm Al_2O_3 powder, washed with deionized water, and then sonicated in ultrapure water for 5 min. In general, 10 μL of a dimethyl sulfoxide dispersion was prepared, which included 1 mg P*p*PD/Fe_3O_4 nanocomposite or Lac-P*p*PD/Fe_3O_4 nanocomposite, then it was spread onto the surface of the freshly cleaned Pt electrode to prepare a thin film, which was allowed to dry at room temperature for 1 h. Electrochemical measurements were performed at room temperature using a three-electrode system with film-immobilized Pt electrode as the working electrode, an Ag/AgCl reference electrode, and a bare Pt counter electrode. Sodium acetate buffer solution (50 mM, pH 4.0) was used as the electrolyte solution.

2.8. Removal of RB-19 by Free and Immobilized Lac and Repeated Use

The removal rate of RB-19 was determined by measuring the absorbance of test samples by spectrophotometry at the maximum absorbance wavelength of the dye (592 nm). The batch dye removal was carried out in 10 mL reaction mixtures containing 12 $mg \cdot L^{-1}$ dye prepared in sodium acetate buffer solution (50 mM, pH 4.0) and 0.5 $U \cdot mL^{-1}$ free or immobilized Lac. The mixtures were incubated in the dark at 25 °C for 2 h. At regular intervals, the treated samples were centrifuged

(9000× g for 5 min) and then the supernatants were recovered and subjected to spectrophotometric analysis to determine their content of RB-19. The magnetic biocatalysts were separated from the reaction broth using a magnet at the same time interval. The dye removal at different time intervals was determined using two different controls, namely heat-inactivated free enzyme and immobilized Lac, which were incubated at 100 °C for 15 min. The capacity of immobilized Lac for repeated dye removal was evaluated over eight cycles. After each reaction cycle, the immobilized Lac was washed several times with the buffer solution and fed into a new cycle. Dye removal (%) was calculated based on the following formula: Dye removal (%) = $(A_0 - A_t)/A_0$, where A_0 is the initial absorbance of the dye and A_t is the absorbance at the measured incubation time point. All experiments were performed in triplicate. Data presented in the figures correspond to mean values with standard errors.

2.9. Measurements

The morphologies of the composites were confirmed by transmission electron microscopy (TEM; model 9000, Hitachi, Tokyo, Japan). Fourier transform infrared spectroscopy (FT-IR) analysis was carried out using a Tensor 27 spectrometer (Bruker, Karlsrohe, Germany). The electrochemical measurements were carried out on a PGSTAT302 Autolab B.V. instrument (Metrohm, Herisau, Switzerland) with a scan range of −2 to 2 V and a scan rate of 5 mV/s. Lac activity and dye removal were measured using a UV-1700 spectrophotometer (Shimadzu, Kyoto, Japan).

3. Results and Discussion

3.1. TEM Imaging and FT-IR Analysis

Representative TEM images of Fe_3O_4 nanoparticles are shown in Figure 2a. Fe_3O_4 magnetic particles were found to have a mean diameter of ~20 nm and to be rod-like in shape. As shown in Figure 2b, the TEM image indicated that the synthesized P*p*PD polymers formed nanofibrous mats, which were amorphous as determined by their electron diffraction patterns. Similar results have been reported for polyaniline/Fe_3O_4 nanocomposite [24].

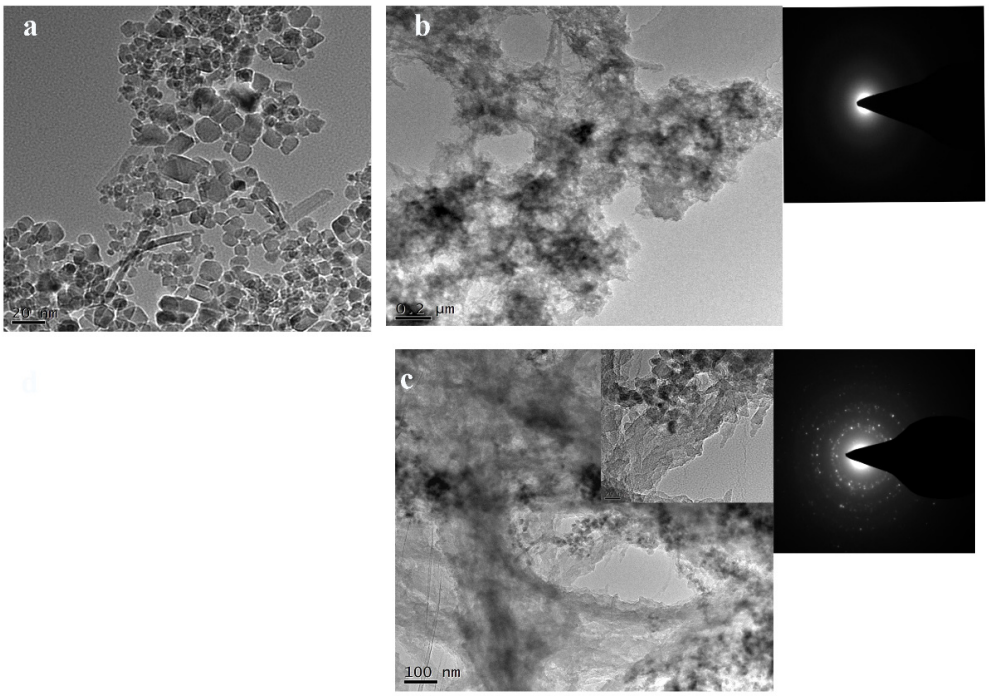

Figure 2. TEM (transmission electron microscopy) and electron diffraction patterns of (**a**) Fe_3O_4; (**b**) P*p*PD; and (**c**) P*p*PD/Fe_3O_4.

The P*p*PD fibers were observed to be randomly cross-linked, and the magnetic particles were aggregated with the fibers (Figure 2c). The TEM image of the P*p*PD/Fe_3O_4 composites was similar to that of the P*p*PD fibers, but small light dots were observed on the composite, which were absent from the image of P*p*PD fibers, suggesting that Fe_3O_4 magnetic particles were embedded into the P*p*PD nanofibrous mats. It has been reported that there is a strong interaction between the quinoid rings of P*p*PD and Fe_3O_4 nanoparticles that enhances the formation of P*p*PD/Fe_3O_4 nanostructures [25]. The P*p*PD/Fe_3O_4 composites could be efficiently separated from the solution using a magnet.

The FT-IR spectra of the nanocomposites are shown in Figure 3. As seen in Figure 3a,b, a broad peak at around 3413 cm^{-1} corresponded to the N-H stretching vibration of the secondary amine group in the polymer chain [24]. The peak at 1613 cm^{-1} was attributed to the stretching vibrations of benzenoid rings, and the bands at 1355 cm^{-1} and 1230 cm^{-1} corresponded to C-N stretching vibration with aromatic conjugation [26]. Besides the above bands, a band at 572 cm^{-1}, which was attributed to Fe_3O_4, was clearly observed in Figure 3a,c, indicating that Fe_3O_4 magnetic nanoparticles existed in the newly synthesized nanocomposite [27]. In brief, these absorption bands confirmed the successful synthesis of the P*p*PD/Fe_3O_4 composite, in agreement with the findings of TEM imaging.

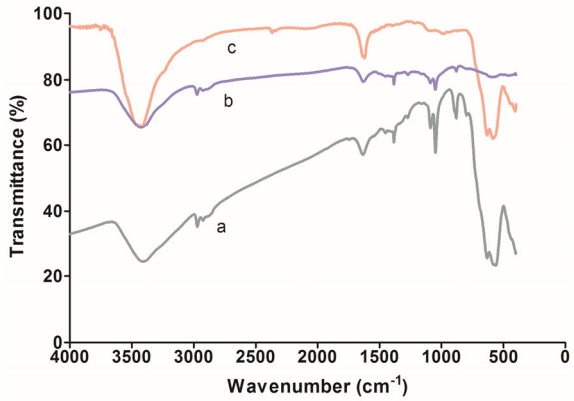

Figure 3. FT-IR (fourier transform infrared spectroscopy) spectra of (**a**) P*p*PD/Fe_3O_4 nanocomposites, (**b**) P*p*PD and (**c**) Fe_3O_4.

3.2. Effects of pH and Temperature on Lac Enzyme Activity

A schematic illustration of Lac immobilization on the P*p*PD/Fe_3O_4 nanocomposites is shown in Figure 4. Under the optimized immobilization conditions, the maximum enzyme load was about 120 mg Lac/g nanocomposite and the maximum retention was about 80% of the original Lac activity. The effect of pH on the activity of the free and immobilized Lac is shown in Figure 5a. According to the experimental results, the optimum reaction pH of free Lac was approximately 4.0, which was consistent with the results of D'Annibale et al. [28]. However, the optimal pH of immobilized Lac showed a slight shift to 3.5. The activity of the immobilized Lac was higher than that of the free Lac in the pH range of 2.0–6.0, which was attributed to the unique electronic properties of P*p*PD. It was previously reported that P*p*PD is a conducting polymer and that the electrochemical process of P*p*PD involves proton transfer [29]. Under acid conditions, the protonation of P*p*PD improved its conductivity property, which was propitious for electron transfer between the enzyme, carrier, and substrates. This resulted in an enhancement of the activity of immobilized Lac, compared with that of free Lac.

The effects of temperature on the activities of free and immobilized Lac are shown in Figure 5b. The relative activities of both forms of Lac clearly increased with the initial increases in temperature, and then decreased with the further increases in temperature. The optimum temperature for the activity of free Lac was 60 °C, while that for the activity of immobilized Lacs was 65 °C. Immobilized Lac exhibited higher stability than free Lac did at higher temperatures. The reason may be that

the P*p*PD/Fe_3O_4 nanocomposite support limited the conformational changes in enzyme molecules, protecting them to some degree from deactivation at high temperatures.

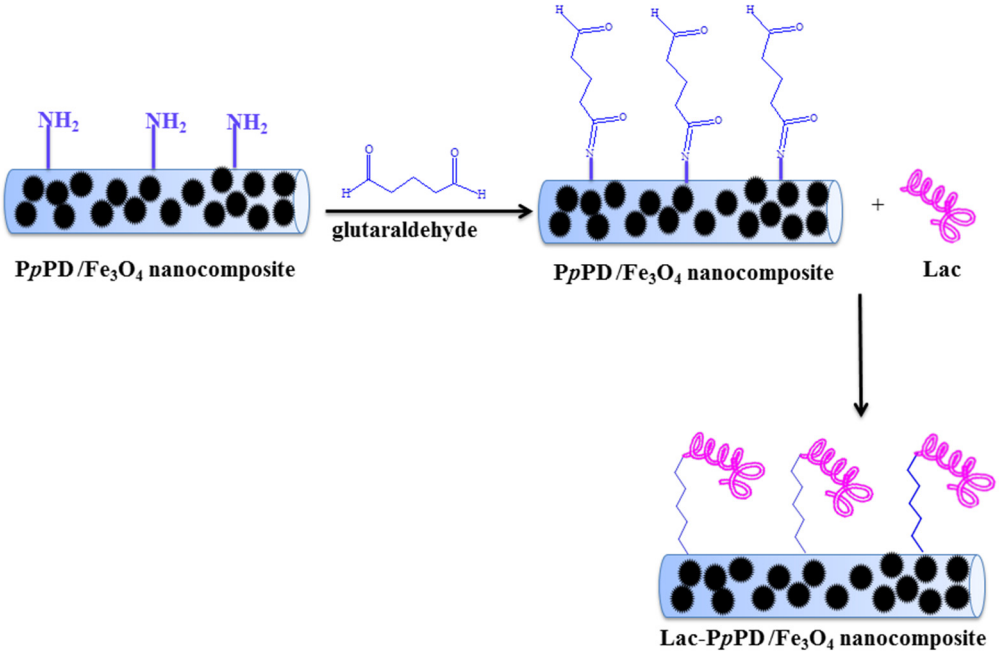

Figure 4. Schematic illustration of Lac immobilization on P*p*PD/Fe_3O_4 nanocomposite.

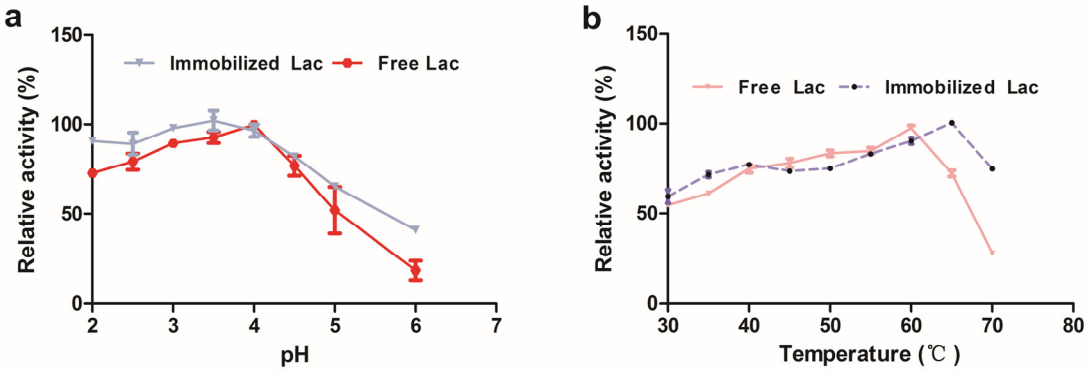

Figure 5. Effects of (**a**) pH and (**b**) temperature on Lac activity.

3.3. Stability Analysis

Figure 6a shows the storage stabilities of immobilized and free Lac. With an increasing storage time, the relative activities of free and immobilized Lac decreased, but free Lac was more rapidly inactivated than immobilized Lac. Free Lac lost 70% of its activity after incubation at 4 °C for 30 days, whereas immobilized Lac lost less than 40% of its activity, demonstrating that it had a higher stability in refrigerated storage than free Lac. It is well-known that storage stability is an important advantage of immobilized enzymes for application in bioprocesses. Figure 6b presents the thermal stability of immobilized Lac. It can be seen that the thermal stability of immobilized Lac on the P*p*PD/Fe_3O_4 nanocomposite was improved to a certain degree. Enzyme immobilization could greatly reduce the costs of using enzymes in practical applications. Immobilized enzymes often have other drawbacks such as low rates of enzyme recovery and recycling [12,30–33]. However, it has been proven that the use of magnetic carriers can dramatically improve the efficiency of enzyme recovery and recycling [34–36]. Thus, the magnetically separable Lac-P*p*PD/Fe_3O_4 nanocomposite may contribute to enzyme recovery and reduce costs. As shown in Figure 6d, Lac immobilized on magnetically separable

P*p*PD nanofibers could be efficiently separated from the reactants using a magnet. After each reaction, the immobilized enzyme was harvested and the recovery of enzyme activity was determined. With an increasing number of use and recovery cycles, the activity of the immobilized Lac gradually decreased owing to inactivation and product loss during each run (Figure 6c). However, more than 75% of its initial activity was retained after eight cycles. The activity of immobilized Lac was clearly stabilized compared with that of free Lac. Similar results have been reported for other nanobiocatalysts [37,38].

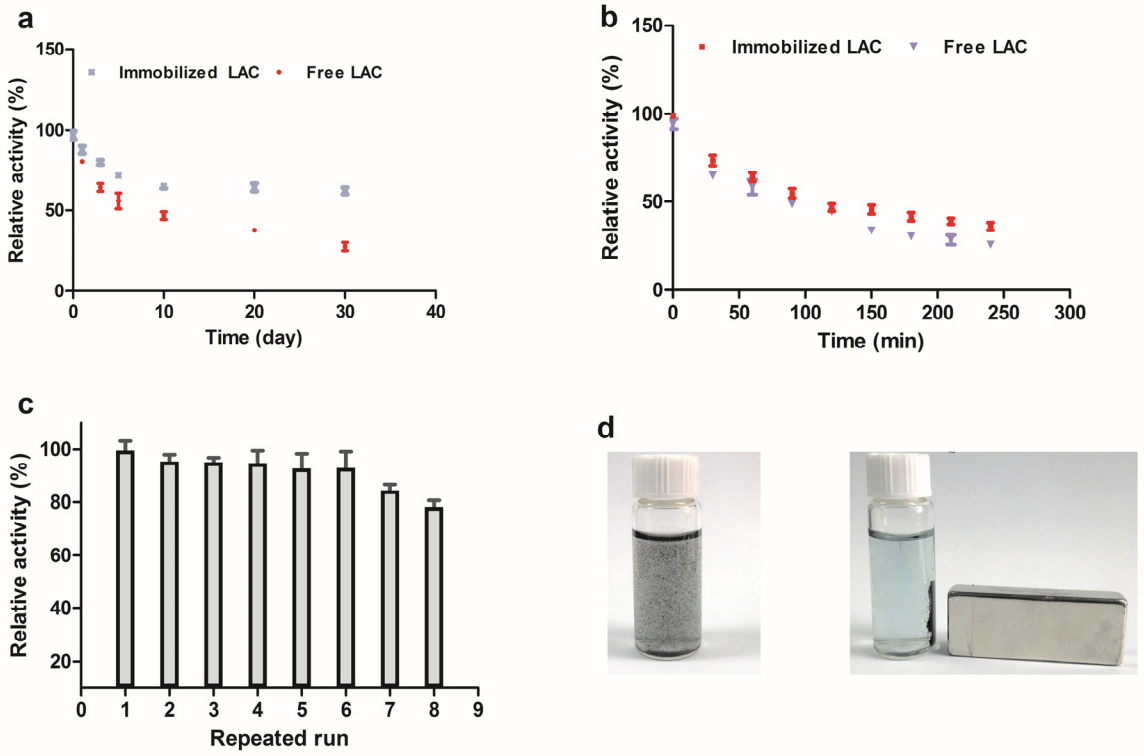

Figure 6. (**a**) Storage stability; (**b**) thermal stability; and (**c**) operational stability of free and immobilized Lac; (**d**) Recovery of immobilized Lac from the solution using a magnet.

The above results showed that the immobilized Lac had a higher stability than its free counterpart. The improved storage and operational stabilities of the immobilized Lac can be attributed to the covalent bonding between the Lac and P*p*PD nanofibers, which improves the enzyme's stability against conformational denaturation under extreme conditions.

3.4. Removal of RB-19

Figure 7 shows the removal of RB-19 by free Lac, immobilized Lac, and carrier (P*p*PD/Fe_3O_4 nanocomposite without Lac) versus time. For immobilized Lac, the removal rate increased rapidly during the first 1 h of treatment and reached 80%. In comparison, the removal efficiency of dye by free Lac only reached 20%. For the carrier, approximately 40% dye removal was obtained in the first 1 h of incubation, and subsequently no significant increase was found. The primary charge on the surface of P*p*PD/Fe_3O_4 nanocomposite was positive at pH 4. Thus, the adsorption of dye on the carrier was partly attributed to ionic electrostatic attractions between the positively charged sites of the carrier surface and the negative sulfonyl ($-SO_3$) groups of dye molecules (Figure 1). Additionally, other adsorption mechanisms such as hydrogen bonding may play a partial role, which may be due to the interactions of groups on the surface of carrier with groups of the RB19 molecule [39]. The dye removal efficiency of immobilized Lac (80%) was clearly higher than that of free Lac under the same conditions, and was even higher than the sum of dye removal by free Lac and the carrier (60%), which can be attributed to two causes. The first is the dye adsorption by the carrier that contributes to

dye removal. The second is increments in solution conductivity brought about by the immobilization of Lac on P*p*PD/Fe_3O_4 nanocomposite, which may be an important factor affecting the removal efficiency. Figure 8 shows that the current of the immobilized Lac-P*p*PD/Fe_3O_4 nanocomposite was higher than that of the carrier without Lac, suggesting that electron transfer occurs between Lac and the P*p*PD fiber. Figure 9 shows the schematic illustration of the interaction mechanisms between Lac, P*p*PD fiber, and RB-19. It can be speculated that the conducting P*p*PD/Fe_3O_4 fiber mat may act as a "molecular wire" and provide effective channels for electron transfer. After the RB-19 molecules were adsorbed to the P*p*PD/Fe_3O_4 nanocomposite, the carrier may promote electron transfer from the redox centers of Lac to the dye and enhance the catalytic activity of Lac [40,41]. Similar results have been reported for catalase covalently bound to electrospun nanofiber meshes filled with carbon nanotubes [40]. It was also reported that the conducting carbon nanotubes were able to promote direct electron transport from redox enzymes such as ascorbate oxidase, peroxidase, and Lac [38,40–46]. Therefore, P*p*PD/Fe_3O_4 nanocomposite may also be suitable for enzyme immobilization, especially for redox enzymes.

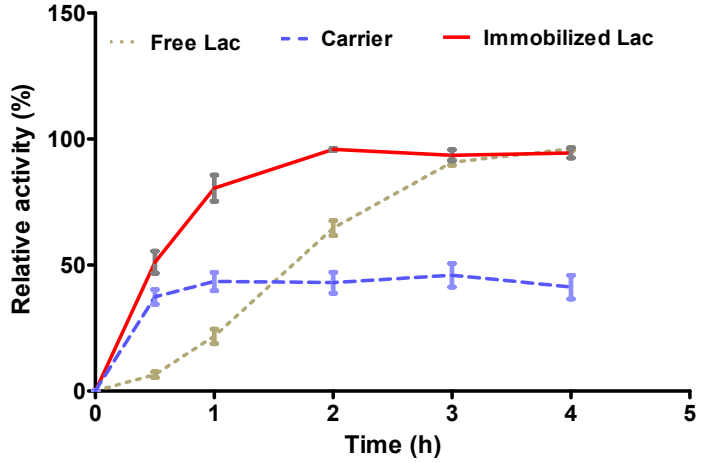

Figure 7. Removal of dye by free Lac, immobilized Lac, and carrier versus time.

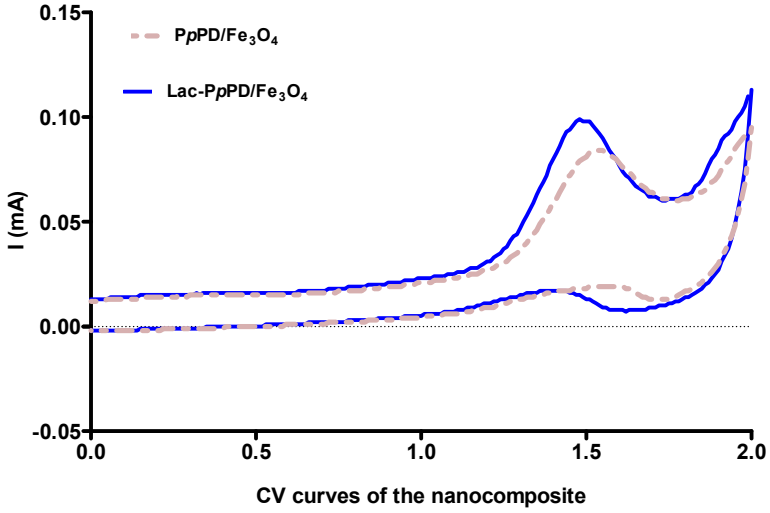

Figure 8. Cyclic voltammetry curves of the P*p*PD/Fe_3O_4 and Lac-P*p*PD/Fe_3O_4 nanocomposites.

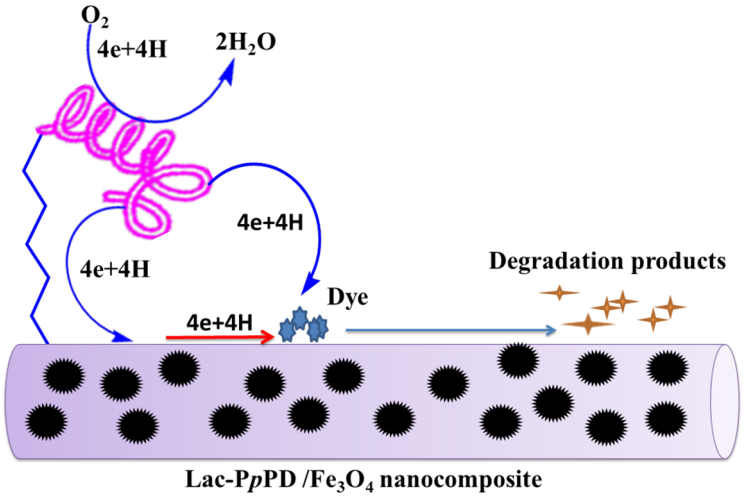

Figure 9. Proposed reaction scheme for dye removal catalyzed by Lac immobilized on P*p*PD/Fe_3O_4.

The reusability of immobilized enzymes is important because of its influence on processing costs in wastewater treatment industries [47]. Figure 10 shows that when the immobilized enzyme was subjected to repeated use and recovery cycles, for the first two cycles, the percentage of dye removal by Lac-P*p*PD/Fe_3O_4 remained the same (90%), and then the recovery efficiency decreased gradually with every cycle, reaching 43% at the eighth cycle. The decreased dye removal efficiency may be related to several factors. First, the enzyme may be inactivated or inhibited by the accumulation of dye degradation products [48]. Second, mass transfer limitations may be induced by dye or metabolite adsorption to the P*p*PD/Fe_3O_4 carrier [49,50]. Moreover, during the catalytic reaction, some of the Fe_3O_4 nanoparticles were found to be released from the P*p*PD/Fe_3O_4 nanocomposite due to vigorous stirring, leading to a reduction in the magnetic force of the carriers. Thus, the immobilized Lac may have partly been lost along with carrier molecules that had lost their magnetism during separation of the immobilized enzyme from the reaction solution using a magnet. The loss of Fe_3O_4 nanoparticles from the nanocomposite will be a challenge for the practical application of Lac-P*p*PD/Fe_3O_4. This problem may be resolved by covalently binding Fe_3O_4 nanoparticles with P*p*PD polymers.

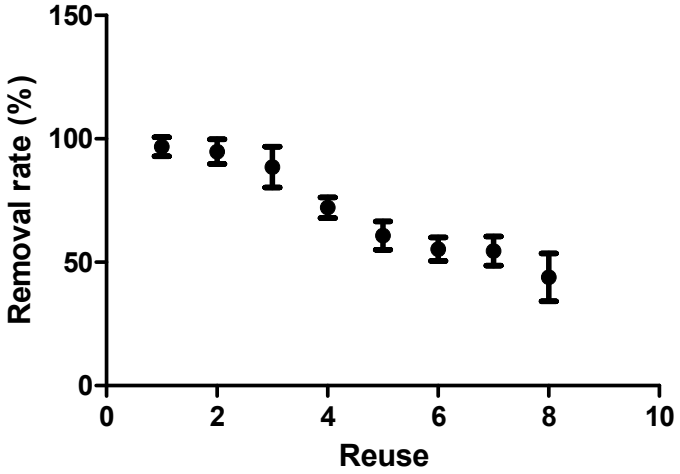

Figure 10. Reusability of the immobilized laccase.

4. Conclusions

In conclusion, we have successfully fabricated P*p*PD/Fe_3O_4 nanocomposite with a high electrical conductivity for use as a carrier for enzyme immobilization. The morphology and chemical structure

of the nanocomposite were characterized using TEM and FT-IR. Both the pH and temperature optima of immobilized Lac showed a slight shift compared with those of free Lac, and the immobilized Lac exhibited a higher activity under conditions of acidic pH. Moreover, the immobilized Lac on P*p*PD/Fe_3O_4 nanofibers showed excellent characteristics, such as high storage, thermal and operational stabilities, easy recovery, and high dye removal efficiency. These advantageous characteristics were related to the electrical conductivity and biocompatible microenvironment provided by the P*p*PD. Our results indicated that P*p*PD/Fe_3O_4 nanocomposite may be an appropriate carrier for enzyme immobilization. Lac-P*p*PD/Fe_3O_4 has potential applications in dye wastewater treatment.

Acknowledgments: This research was kindly supported by the Doctoral Innovation Fund of Xinxiang Medical University, Nature Science Plan Program from the education department of Henan province (12B180030) and the National Natural Science Foundation of China (No. U1304302).

Author Contributions: Youxun Liu and Juan Huang had the original idea for the study. Juan Huang and Mingyang Yan were responsible for data collection and carried out the analyses. Youxun Liu and Yuanyuan Geng drafted the manuscript, which was revised by all authors. All authors read and approved the final manuscript.

Conflicts of Interest: The authors declare no conflict of interest.

References

1. Rivera-Hoyos, C.M.; Morales-Álvarez, E.D.; Poutou-Piñales, R.A.; Pedroza-Rodríguez, A.M.; Rodríguez-Vázquez, R.; Delgado-Boada, J.M. Fungal laccases. *Fungal Biol. Rev.* **2013**, *27*, 67–82. [CrossRef]
2. Jones, S.M.; Solomon, E.I. Electron transfer and reaction mechanism of laccases. *Cell. Mol. Life Sci.* **2015**, *72*, 869–883. [CrossRef] [PubMed]
3. Senthivelan, T.; Kanagaraj, J.; Panda, R.C. Recent trends in fungal laccase for various industrial applications: An eco-friendly approach—A review. *Biotechnol. Bioprocess Eng.* **2016**, *21*, 19–38. [CrossRef]
4. Mogharabi, M.; Faramarzi, M.A. Laccase and laccase-mediated systems in the synthesis of organic compounds. *Adv. Synth. Catal.* **2014**, *356*, 897–927. [CrossRef]
5. Roth, S.; Spiess, A.C. Laccases for biorefinery applications: A critical review on challenges and perspectives. *Bioprocess Biosyst. Eng.* **2015**, *38*, 2285–2313. [CrossRef] [PubMed]
6. Cañas, A.I.; Camarero, S. Laccases and their natural mediators: Biotechnological tools for sustainable eco-friendly processes. *Biotechnol. Adv.* **2010**, *28*, 694–705. [CrossRef] [PubMed]
7. Woodward, S.; Ellouz, M.; Dhouib, A. Decolourization and detoxification of textile industry wastewater by the laccase-mediator system. *J. Hazard. Mater.* **2009**, *175*, 802–808.
8. Zucca, P.; Cocco, G.; Sollai, F.; Sanjust, E. Fungal laccases as tools for biodegradation of industrial dyes. *Biocatalysis* **2016**, *1*, 82–108. [CrossRef]
9. Ursoiu, A.; Paul, C.; Kurtán, T.; Péter, F. Sol-gel entrapped Candida antarctica lipase B—A biocatalyst with excellent stability for kinetic resolution of secondary alcohols. *Molecules* **2012**, *17*, 13045–13061. [CrossRef] [PubMed]
10. Ansari, S.A.; Husain, Q. Potential applications of enzymes immobilized on/in nano materials: A review. *Biotechnol. Adv.* **2012**, *30*, 512–523. [CrossRef] [PubMed]
11. Buthe, A.; Wu, S.; Ping, W. Nanoporous silica glass for the immobilization of interactive enzyme systems. *Methods Mol. Biol.* **2011**, *679*, 37–48. [PubMed]
12. Hwang, E.T.; Gu, M.B. Enzyme stabilization by nano/microsized hybrid materials. *Eng. Life Sci.* **2013**, *13*, 49–61. [CrossRef]
13. Wang, Z.-G.; Wan, L.-S.; Liu, Z.-M.; Huang, X.-J.; Xu, Z.-K. Enzyme immobilization on electrospun polymer nanofibers: An overview. *J. Mol. Catal. B Enzym.* **2009**, *56*, 189–195. [CrossRef]
14. Ba, S.; Arsenault, A.; Hassani, T.; Jones, J.P.; Cabana, H. Laccase immobilization and insolubilization: From fundamentals to applications for the elimination of emerging contaminants in wastewater treatment. *Crit. Rev. Biotechnol.* **2012**, *33*, 404–418. [CrossRef] [PubMed]
15. Lalaoui, N.; Elouarzaki, K.; Le Goff, A.; Holzinger, M.; Cosnier, S. Efficient direct oxygen reduction by laccases attached and oriented on pyrene-functionalized polypyrrole/carbon nanotube electrodes. *Chem. Commun.* **2013**, *49*, 9281–9283. [CrossRef] [PubMed]

16. Xiao, B.-L.; Hong, J.; Gao, Y.-F.; Yang, T.; Moosavi-Movahedi, A.A.; Ghourchian, H. Direct electron transfer of horseradish peroxidase on a functional nanocomplex modified glassy carbon electrode. *Biomed. Mater. Eng.* **2014**, *24*, 1079–1084. [PubMed]
17. Patil, S.R.; Choudhary, A.S.; Sekar, N. Disperse styryl and azo dyes for polyester and nylon fibre: Synthesis, optical properties having the 1,2,4-triketo naphthoquinone skeleton. *Fibers Polym.* **2015**, *16*, 1068–1074. [CrossRef]
18. Parmar, N.; Shukla, S.R. Microbial Decolorization of reactive dye solutions. *CLEAN-Soil Air Water* **2015**, *43*, 1426–1432. [CrossRef]
19. Zhuo, R.; He, F.; Zhang, X.; Yang, Y. Characterization of a yeast recombinant laccase rLAC-EN3-1 and its application in decolorizing synthetic dye with the coexistence of metal ions and organic solvents. *Biochem. Eng. J.* **2015**, *93*, 63–72. [CrossRef]
20. Chhabra, M.; Mishra, S.; Sreekrishnan, T.R. Immobilized laccase mediated dye decolorization and transformation pathway of azo dye acid red. *J. Environ. Health Sci. Eng.* **2015**, *13*, 1–9. [CrossRef] [PubMed]
21. Yang, S.; Liu, D.; Liao, F.; Guo, T.; Wu, Z.; Zhang, T. Synthesis, characterization, morphology control of poly (*p*-phenylenediamine)-Fe_3O_4 magnetic micro-composite and their application for the removal of $Cr_2O_7^{2-}$ from water. *Synth. Met.* **2012**, *162*, 2329–2336. [CrossRef]
22. Yang, S.; Ye, C.; Song, X.; He, L.; Yan, S.; Liao, F. Theoretical calculations based synthesis of poly(*p*-phenylenediamine)-Fe_3O_4 composite: A magnetically recyclable photocatalyst with highly selectivity for acid dyes. *RSC Adv.* **2014**, *4*, 54810–54818. [CrossRef]
23. Cao, J.; Wang, Y.; Yu, J.; Xia, J.; Zhang, C.; Yin, D.; Häfeli, U.O. Preparation and radiolabeling of surface-modified magnetic nanoparticles with rhenium-188 for magnetic targeted radiotherapy. *J. Magn. Magn. Mater.* **2004**, *277*, 165–174. [CrossRef]
24. Zhang, Z.; Wan, M.; Wei, Y. Electromagnetic functionalized polyaniline nanostructures. *Nanotechnology* **2005**, *16*, 2827. [CrossRef]
25. Lakouraj, M.M.; Zare, E.N.; Moghadam, P.N. Synthesis of novel conductive poly(*p*-phenylenediamine)/Fe_3O_4 nanocomposite via emulsion polymerization and investigation of antioxidant activity. *Adv. Polym. Technol.* **2014**, *33*, 509–516.
26. Baghayeri, M.; Zare, E.N.; Lakouraj, M.M. A simple hydrogen peroxide biosensor based on a novel electro-magnetic poly(*p*-phenylenediamine)@Fe_3O_4 nanocomposite. *Biosens. Bioelectron.* **2014**, *55*, 259–265. [CrossRef] [PubMed]
27. Ghosh, R.; Pradhan, L.; Devi, Y.P.; Meena, S.S.; Tewari, R.; Kumar, A.; Sharma, S.; Gajbhiye, N.S.; Vatsa, R.K.; Pandey, B.N. Induction heating studies of Fe_3O_4 magnetic nanoparticles capped with oleic acid and polyethylene glycol for hyperthermia. *J. Mater. Chem.* **2011**, *21*, 13388–13398. [CrossRef]
28. Zhao, J.; Kwan, H.S. Characterization, molecular cloning, and differential expression analysis of laccase genes from the edible mushroomLentinula edodes. *Appl. Environ. Microbiol.* **1999**, *65*, 4908–4913. [PubMed]
29. Baghayeri, M. Glucose sensing by a glassy carbon electrode modified with glucose oxidase and a magnetic polymeric nanocomposite. *RSC Adv.* **2015**, *5*, 18267–18274. [CrossRef]
30. Sheldon, R.A. Enzyme immobilization: The quest for optimum performance. *Adv. Synth. Catal.* **2007**, *349*, 1289–1307. [CrossRef]
31. Mateo, C.; Palomo, J.M.; Fernandez-Lorente, G.; Guisan, J.M.; Fernandez-Lafuente, R. Improvement of enzyme activity, stability and selectivity via immobilization techniques. *Enzyme Microb. Technol.* **2007**, *40*, 1451–1463. [CrossRef]
32. Hanefeld, U.; Gardossi, L.; Magner, E. Understanding enzyme immobilisation. *Chem. Soc. Rev.* **2009**, *38*, 453–468. [CrossRef] [PubMed]
33. Brady, D.; Jordaan, J. Advances in enzyme immobilisation. *Biotechnol. Lett.* **2009**, *31*, 1639–1650. [CrossRef] [PubMed]
34. Sheldon, R.A. Characteristic features and biotechnological applications of cross-linked enzyme aggregates (CLEAs). *Appl. Microbiol. Biotechnol.* **2011**, *92*, 467–477. [CrossRef] [PubMed]
35. Xie, W.; Ma, N. Immobilized lipase on Fe_3O_4 nanoparticles as biocatalyst for biodiesel production. *Energy Fuels* **2009**, *23*, 1347–1353. [CrossRef]
36. Guo, Z.; Bai, S.; Sun, Y. Preparation and characterization of immobilized lipase on magnetic hydrophobic microspheres. *Enzyme Microb. Technol.* **2003**, *32*, 776–782. [CrossRef]

37. Huang, X.-J.; Yu, A.-G.; Xu, Z.-K. Covalent immobilization of lipase from Candida rugosa onto poly (acrylonitrile-co-2-hydroxyethyl methacrylate) electrospun fibrous membranes for potential bioreactor application. *Bioresour. Technol.* **2008**, *99*, 5459–5465. [CrossRef] [PubMed]
38. Dai, Y.; Yin, L.; Niu, J. Laccase-carrying electrospun fibrous membranes for adsorption and degradation of PAHs in shoal soils. *Environ. Sci. Technol.* **2011**, *45*, 10611–10618. [CrossRef] [PubMed]
39. Khoshhesab, Z.M.; Ahmadi, M. Removal of reactive blue 19 from aqueous solutions using NiO nanoparticles: Equilibrium and kinetic studies. *Desalination Water Treat.* **2016**, *57*, 1–12. [CrossRef]
40. Zhao, Y.-D.; Zhang, W.-D.; Chen, H.; Luo, Q.-M.; Li, S.F.Y. Direct electrochemistry of horseradish peroxidase at carbon nanotube powder microelectrode. *Sens. Actuators B Chem.* **2002**, *87*, 168–172. [CrossRef]
41. Feng, W.; Wu, Z.; Li, Y.; Feng, Y.; Yuan, X. The fabrication and electrochemical properties of electrospun nanofibers of a multiwalled carbon nanotube grafted by chitosan. *Nanotechnology* **2008**, *19*, 235–243. [CrossRef] [PubMed]
42. Wang, Z.-G.; Ke, B.-B.; Xu, Z.-K. Covalent immobilization of redox enzyme on electrospun nonwoven poly (acrylonitrile-co-acrylic acid) nanofiber mesh filled with carbon nanotubes: A comprehensive study. *Biotechnol. Bioeng.* **2007**, *97*, 708–720. [CrossRef] [PubMed]
43. Wan, L.-S.; Ke, B.-B.; Wu, J.; Xu, Z.-K. Catalase immobilization on electrospun nanofibers: Effects of porphyrin pendants and carbon nanotubes. *J. Phys. Chem. C* **2007**, *111*, 14091–14097. [CrossRef]
44. Wang, Z.; Li, M.; Su, P.; Zhang, Y.; Shen, Y.; Han, D.; Ivaska, A.; Niu, L. Direct electron transfer of horseradish peroxidase and its electrocatalysis based on carbon nanotube/thionine/gold composites. *Electrochem. Commun.* **2008**, *10*, 306–310. [CrossRef]
45. Liu, M.; Wen, Y.; Li, D.; He, H.; Xu, J.; Liu, C.; Yue, R.; Lu, B.; Liu, G. Electrochemical immobilization of ascorbate oxidase in poly(3,4-ethylenedioxythiophene)/multiwalled carbon nanotubes composite films. *J. Appl. Polym. Sci.* **2011**, *122*, 1142–1151. [CrossRef]
46. Bourourou, M.; Elouarzaki, K.; Lalaoui, N.; Agnès, C.; Le Goff, A.; Holzinger, M.; Maaref, A.; Cosnier, S. Supramolecular immobilization of laccase on carbon nanotube electrodes functionalized with (methylpyrenylaminomethyl) anthraquinone for direct electron reduction of oxygen. *Chem. Eur. J.* **2013**, *19*, 9371–9375. [CrossRef] [PubMed]
47. Karam, J.; Nicell, J.A. Potential applications of enzymes in waste treatment. *J. Chem. Technol. Biotechnol.* **1997**, *69*, 141–153. [CrossRef]
48. Russo, M.E.; Giardina, P.; Marzocchella, A.; Salatino, P.; Sannia, G. Assessment of anthraquinone-dye conversion by free and immobilized crude laccase mixtures. *Enzyme Microb. Technol.* **2008**, *42*, 521–530. [CrossRef]
49. Cabana, H.; Jones, J.P.; Agathos, S.N. Utilization of cross-linked laccase aggregates in a perfusion basket reactor for the continuous elimination of endocrine-disrupting chemicals. *Biotechnol. Bioeng.* **2009**, *102*, 1582–1592. [CrossRef] [PubMed]
50. Lloret, L.; Hollmann, F.; Eibes, G.; Feijoo, G.; Moreira, M.T.; Lema, J.M. Immobilisation of laccase on Eupergit supports and its application for the removal of endocrine disrupting chemicals in a packed-bed reactor. *Biodegradation* **2012**, *23*, 373–386. [CrossRef] [PubMed]